

# Neural cell adhesion molecule promotes accumulation of TGN organelles at sites of neuron-to-neuron contacts

Vladimir Sytnyk,<sup>1,2</sup> Iryna Leshchyns'ka,<sup>1</sup> Markus Delling,<sup>1</sup> Galina Dityateva,<sup>1</sup> Alexander Dityatev,<sup>1</sup> and Melitta Schachner<sup>1</sup>

<sup>1</sup>Zentrum für Molekulare Neurobiologie, Universität Hamburg, D-20246 Hamburg, Germany

<sup>2</sup>Laboratory for Biophysics and Bioelectronics, Dnepropetrovsk State University, 49050 Dnepropetrovsk, Ukraine

**T**ransformation of a contact between axon and dendrite into a synapse is accompanied by accumulation of the synaptic machinery at this site, being delivered in intracellular organelles mainly of TGN origin. Here, we report that in cultured hippocampal neurons, TGN organelles are linked via spectrin to clusters of the neural cell adhesion molecule (NCAM) in the plasma membrane. These com-

plexes are translocated along neurites and trapped at sites of initial neurite-to-neurite contacts within several minutes after initial contact formation. The accumulation of TGN organelles at contacts with NCAM-deficient neurons is reduced when compared with wild-type cells, suggesting that NCAM mediates the anchoring of intracellular organelles in nascent synapses.

## Introduction

Synaptogenesis in the CNS is accompanied by accumulation of synaptic organelles and proteins at the sites of contact between axons and dendrites (Mammen et al., 1997; Rao et al., 1998; Friedman et al., 2000; Lee and Sheng, 2000; Zhai et al., 2001). The culmination of this process is the transformation of the initial contacts into functional synapses. In axons, synaptic proteins are transported within intracellular tubulovesicular membrane aggregates of TGN origin that probably represent synaptic vesicle precursors (Nakata et al., 1998). These precursors then concentrate at sites of contact in parallel with their transformation into synapses (Ahmari et al., 2000). In dendrites, TGN organelles undergo regulated exocytosis and are suggested to mediate the delivery of synaptic proteins to postsynaptic sites (Lledo et al., 1998; Maletic-Savatic and Malinow, 1998; Shi et al., 1999). The question is how these organelles are captured and stabilized at sites of contact that would initiate their transformation into synapses or mediate synaptic rearrangements.

Cell adhesion molecules are probably the best candidates to execute this task. In *Drosophila*, a deficit in the cell adhesion

molecule fasciclin II leads to a loss of synapses (Schuster et al., 1996). In mammals, the neural cell adhesion molecule (NCAM),\* the closest homologue of fasciclin II, accumulates at sites of intercellular contacts, where it has been proposed to stabilize the contact structure (Pollerberg et al., 1986, 1987). The role of NCAM in synaptogenesis was demonstrated in experiments showing a higher number of synapses on NCAM-expressing neurons compared with NCAM-deficient cells in a choice situation in heterogenotypic cocultures of NCAM-deficient and wild-type neurons (Dityatev et al., 2000). NCAM is expressed in three major splicing isoforms: GPI-linked NCAM120 (120 kD) and transmembrane NCAM140 (140 kD) and NCAM180 (180 kD). NCAM180, the isoform with the largest intracellular domain, interacts with spectrin (Pollerberg et al., 1986, 1987) and could provide a direct link to intracellular organelles, such as TGN organelles, which are lined by a spectrin cytoskeleton (De Matteis and Morrow, 1998; Holleran and Holzbaur, 1998; Lippincott-Schwartz, 1998).

Here, we used time-lapse confocal microscopic video recordings, markers of subcellular compartments, and subcellular fractionation to describe an association between NCAM clusters and intracellular aggregates of TGN organelles that are transported en ensemble to initial neuron–neuron contacts.

The online version of this article includes supplemental material.

Address correspondence to Melitta Schachner, Zentrum für Molekulare Neurobiologie, Universität Hamburg, Martinistrasse 52, D-20246 Hamburg, Germany. Tel.: 49-40-42803-6246. Fax: 49-40-42803-6248. E-mail: melitta.schachner@zmnh.uni-hamburg.de

Key words: NCAM; trans-Golgi network; contacts; synapses; hippocampal neurons

\*Abbreviations used in this paper: DIC, differential interference contrast; NCAM, neural cell adhesion molecule.

We demonstrate that NCAM mediates the capture of organelles at initial sites of contact that is followed by the transformation of these contacts into functional synapses.

## Results

### NCAM clusters associate with a subpopulation of intracellular organelles

To study the relationship between localization of intracellular organelles and distribution of NCAM at the neuronal surface, we used differential interference contrast (DIC) microscopy combined with subsequent immunofluorescence analysis. In hippocampal neurons maintained for 1–3 d *in vitro*, intracellular organelles (observed as dark granules by DIC microscopy) were typically localized within neurite swellings of 1–2  $\mu\text{m}$  in diameter. As observed by time-lapse video recording, intracellular organelles underwent rapid intermittent movement along neurites with a speed that reached  $\sim 0.5 \mu\text{m/s}$ . These intracellular aggregates often resembled transport packets as described previously (Ahmari et al., 2000; Washbourne et al., 2002) (Fig. 1 a).

After time-lapse imaging, neurons were fixed and stained with antibodies to NCAM, showing that a subpopulation of organelles that had moved during video recording were colocalized with intensely labeled clusters of NCAM (Fig. 1, a and b). NCAM clusters occupied areas of the plasma membrane of 0.4–2  $\mu\text{m}$  in diameter that covered the plasma membrane over the intracellular organelles. The immunofluorescence intensity associated with NCAM clusters was more than two times higher than the basal level of immunofluorescence along the neurite. Because no detergents were used for immunofluorescence staining, the observed NCAM immunostaining pattern represented plasma membrane, and not intracellular, NCAM localization. In support of this argument, antibodies to tubulin applied in mixture with NCAM antibodies to neurons not treated with Triton X-100 did not give any staining (Fig. 1 b, tubulin, control), whereas antibodies to tubulin applied to cells treated after fixation with 0.25% Triton X-100 yielded a strong and uniform staining of microtubules in soma and neurites (unpublished data). Because intracellular organelles were usually located within varicosities, the question arose whether the apparent peaks of NCAM immunofluorescence intensity associated with organelles were due to the larger diameter of neurites at these sites. To resolve this, we stained neurons with the lipophilic dye DiI, which intercalates into the surface membrane by lateral diffusion. DiI showed a uniform distribution along neurites independently of neurite thickness and presence of varicosities (unpublished data), indicating that the peaks of NCAM immunofluorescence intensity at the cell surface corresponded to a higher density of NCAM at these sites.

### NCAM clusters interact with TGN organelles via spectrin

To identify the composition of intracellular organelles associated with NCAM-immunoreactive clusters, neurons were stained with NCAM antibodies and labeled with antibodies to different organelle-specific markers. To label the TGN

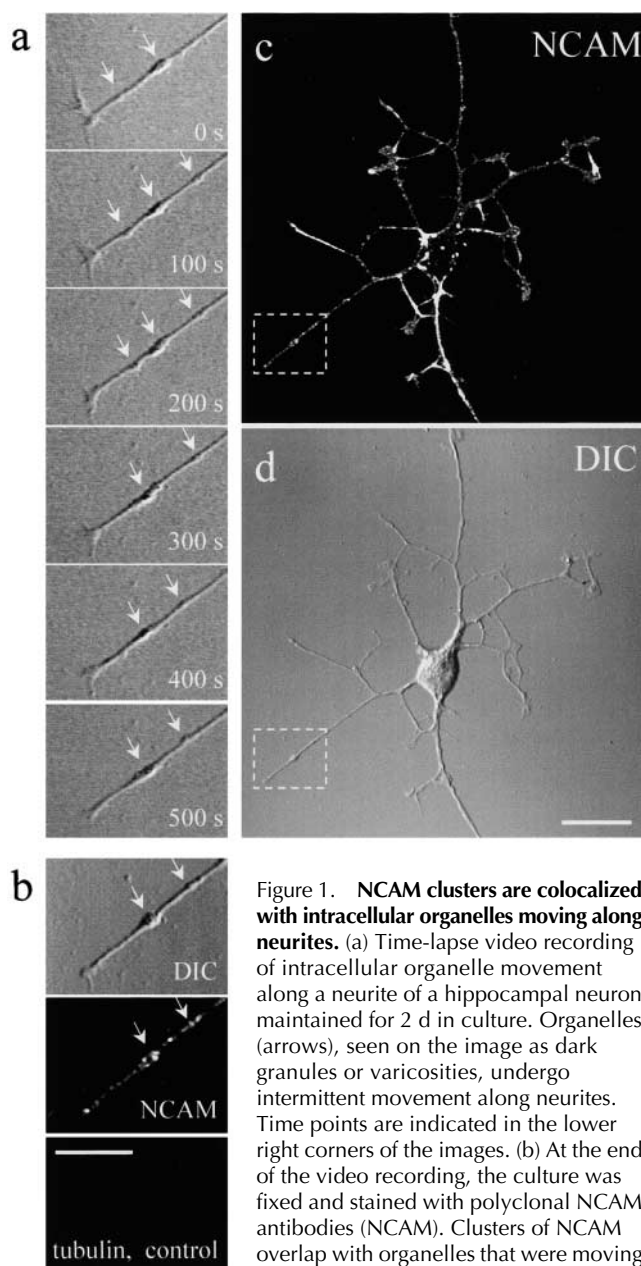


**Figure 1. NCAM clusters are colocalized with intracellular organelles moving along neurites.** (a) Time-lapse video recording of intracellular organelle movement along a neurite of a hippocampal neuron maintained for 2 d in culture. Organelles (arrows), seen on the image as dark granules or varicosities, undergo intermittent movement along neurites. Time points are indicated in the lower right corners of the images. (b) At the end of the video recording, the culture was fixed and stained with polyclonal NCAM antibodies (NCAM). Clusters of NCAM overlap with organelles that were moving during the video recording (arrows, see the corresponding DIC image). Antibodies against tubulin, applied together with NCAM antibodies to control membrane integrity, do not show any staining (tubulin, control). (c and d) Indirect immunofluorescence for NCAM and the corresponding DIC image of the neuron taken for video recording. Brackets show the area taken for the recording. Bars: (b) 10  $\mu\text{m}$  (for a and b); (d) 20  $\mu\text{m}$  (for c and d).

and TGN-derived organelles, we used antibodies to  $\gamma$ -adap-tin (Robinson and Kreis, 1992; Girotti and Banting, 1996). This protein belongs to the AP-1 complex associated with the TGN and clathrin-coated vesicles that bud from the TGN (Robinson and Kreis, 1992; Schmid, 1997; Heilmann et al., 1999) and that are distinct from clathrin-coated endocytic vesicles, which incorporate another adaptor complex, AP-2 (Clague, 1998). Also, we used antibodies to  $\beta$ -COP, a coat protein associated with the TGN and non-clathrin-coated vesicles that bud from the TGN (Robinson and Kreis, 1992). To label endosomal vesicles, we used anti-

and TGN-derived organelles, we used antibodies to  $\gamma$ -adap-tin (Robinson and Kreis, 1992; Girotti and Banting, 1996). This protein belongs to the AP-1 complex associated with the TGN and clathrin-coated vesicles that bud from the TGN (Robinson and Kreis, 1992; Schmid, 1997; Heilmann et al., 1999) and that are distinct from clathrin-coated endocytic vesicles, which incorporate another adaptor complex, AP-2 (Clague, 1998). Also, we used antibodies to  $\beta$ -COP, a coat protein associated with the TGN and non-clathrin-coated vesicles that bud from the TGN (Robinson and Kreis, 1992). To label endosomal vesicles, we used anti-

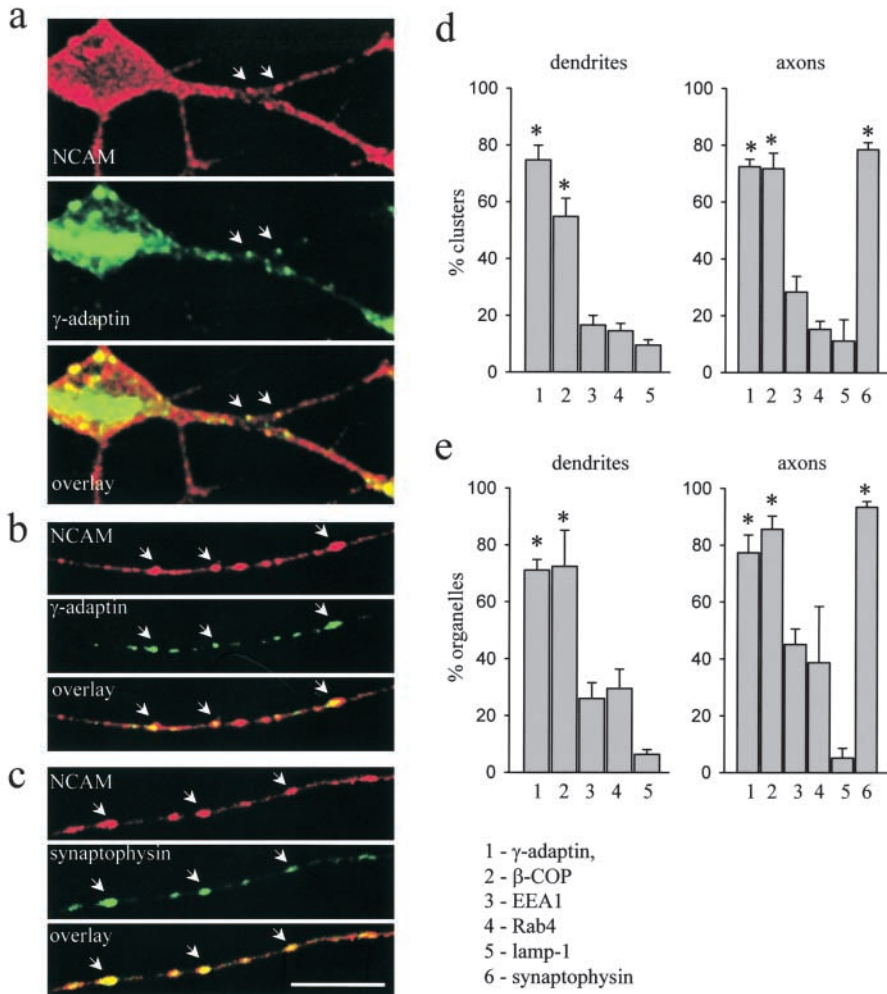


**Figure 2. NCAM clusters are associated with TGN organelles.** (a–c) Double immunofluorescence staining of the hippocampal neurons maintained for 4 d in vitro using antibodies against NCAM,  $\gamma$ -adaptin (a and b), and synaptophysin (c). Neurites considered as dendrites (a) or axons (b and c) are shown. Clusters of NCAM coincide with  $\gamma$ -adaptin-positive organelles and synaptophysin accumulations (arrows). Bar, 10  $\mu$ m. (d and e) Mean percentage of NCAM clusters that overlap with organelles labeled with antibodies against  $\gamma$ -adaptin,  $\beta$ -COP, EEA1, Rab4, lamp-1, and synaptophysin (d) and mean percentage of organelles labeled with antibodies against  $\gamma$ -adaptin,  $\beta$ -COP, EEA1, Rab4, lamp-1, and synaptophysin that overlap with NCAM clusters (e). Data present mean  $\pm$  SEM ( $n > 20$  neurons,  $>200$  organelles). \* $P < 0.01$ , unpaired  $t$  test shows a significant difference between the percentage of NCAM clusters overlapping with  $\gamma$ -adaptin-,  $\beta$ -COP-, and synaptophysin-positive organelles and a significant difference between the percentage of  $\gamma$ -adaptin-,  $\beta$ -COP-, and synaptophysin-positive organelles overlapping with NCAM clusters compared with other markers.

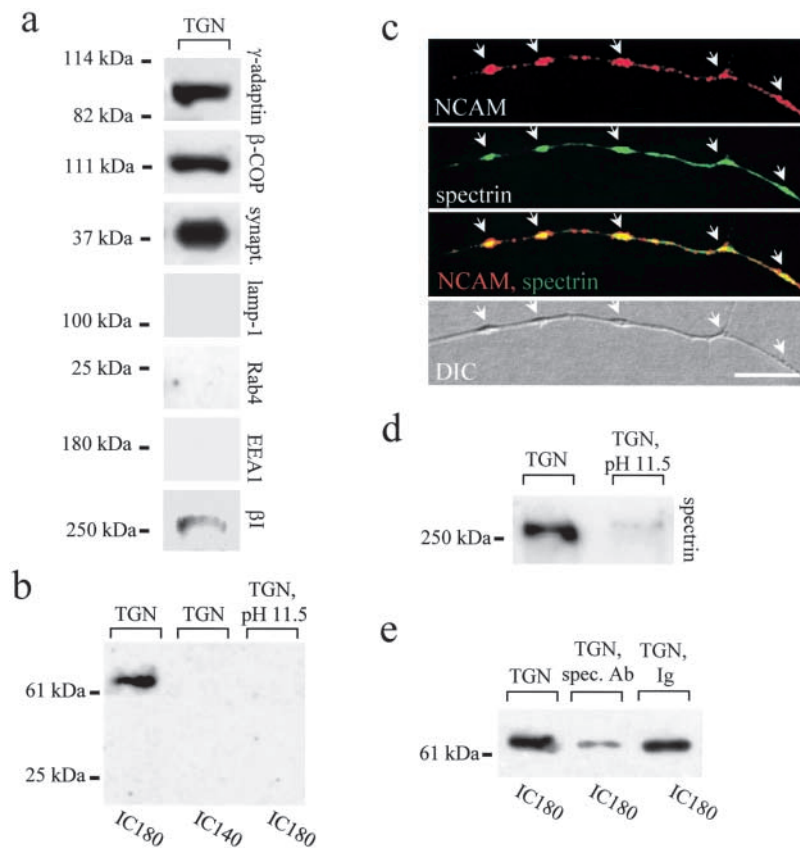
bodies to EEA1, an early endosome-associated protein (Mu et al., 1995), Rab4, characteristic of early and recycling endosomes (Sonnichsen et al., 2000), and lamp-1, a lysosomal membrane glycoprotein (Fukuda, 1991). These markers were highly concentrated in the soma and showed a patchy distribution along neurites. Thick tapering neurites were identified as dendrites, whereas thin neurites of a uniform diameter with multiple varicosities were identified as axons. This classification was verified in a separate set of experiments using the established markers, such as tau and synaptophysin for axons (Ahmari et al., 2000; Paglini et al., 2000) and MAP2b for dendrites (Shafit-Zagardo and Kalcheva, 1998). Along dendrites and axons, NCAM-immunoreactive clusters were significantly more associated with intracellular aggregates containing  $\gamma$ -adaptin- and  $\beta$ -COP-positive organelles than with the other markers, with  $\sim 70\%$  of all NCAM clusters overlapping with  $\gamma$ -adaptin and  $\beta$ -COP immunopositive organelles (Fig. 2, a, b, and d). Approximately 70% of  $\gamma$ -adaptin- and  $\beta$ -COP-positive organelles overlapped with NCAM clusters both in dendrites and axons (Fig. 2 e).  $\gamma$ -Adaptin and  $\beta$ -COP accumulate in the TGN where they mediate budding of two different types of vesicles (Robinson and Kreis, 1992; Heimann et al., 1999). TGN and TGN-derived organelles could form large, up to several micrometers in diameter, vesicular-tubular structures

(Nakata et al., 1998; Toomre et al., 1999, 2000; Polishchuk et al., 2000), which have been shown to transport synapse-specific proteins (Nakata et al., 1998). The synaptic vesicle protein synaptophysin was accumulated in varicosities of neurites (Fig. 2 c), identified as axons by this presynaptic marker. Double immunostaining for NCAM and synaptophysin showed that 80% of all NCAM clusters in axons coincided with synaptophysin clusters, and  $\sim 90\%$  of all synaptophysin clusters overlapped with NCAM clusters (Fig. 2, c–e). Thus, NCAM clusters strongly overlap with TGN and synaptic vesicle markers.

We next studied whether the intracellular domains of NCAM140 or NCAM180 interact with TGN organelles. To this aim, TGN membranes were isolated from the brains of NCAM-deficient mice. NCAM-deficient mice were used instead of wild-type mice to ensure that binding sites for the intracellular domains of NCAM would not be saturated by endogenous NCAM. Immunoblotting confirmed that the isolated membranes were positive for the TGN markers  $\gamma$ -adaptin and  $\beta$ -COP and the synaptic vesicle marker synaptophysin, and negative for the endosomal markers EEA1, Rab4, and lamp-1 (Fig. 3 a). TGN membranes were incubated with the intracellular domains of NCAM140 (IC140) and NCAM180 (IC180), washed, and assayed for IC140 and IC180 binding after separation of the complexes by

**Figure 3. NCAM180 interacts with TGN membranes via spectrin.**

(a) Isolated TGN membranes (TGN) are positive for  $\gamma$ -adaptin,  $\beta$ -COP, and synaptophysin, and negative for lamp-1, Rab4, and EEA1. They also contain  $\beta$ I spectrin labeled with  $\beta$ I-specific antibodies. (b) TGN membranes isolated from the brains of NCAM-deficient mice were incubated with intracellular domains of NCAM140 (IC140) and NCAM180 (IC180), washed, and assayed for IC140 and IC180 binding by immunoblotting with antibodies to NCAM. Immunoblots show that only IC180 interacts with TGN membranes (TGN, IC180), whereas IC140 does not show any binding and precipitation (TGN, IC140). IC180 does not precipitate with TGN membranes extracted at pH 11.5 (TGN, pH 11.5, IC180). (c) Clusters of NCAM overlap with spectrin accumulations (arrows). Hippocampal neurons were maintained for 3 d *in vitro*. Bar, 10  $\mu$ m. (d) Spectrin is removed from TGN membranes by extraction at pH 11.5. (e) TGN membranes isolated from the brains of NCAM-deficient mice were incubated with polyclonal antibodies to spectrin and nonimmune immunoglobulins. Then, untreated and treated TGN membranes were assayed for IC180 binding. Immunoblots show that spectrin polyclonal antibodies significantly reduce binding of IC180 (TGN, spec. Ab, IC180), when compared with untreated TGN membranes (TGN, IC180) or TGN membranes incubated with nonimmune immunoglobulins (TGN, Ig, IC180).



SDS-PAGE and immunoblotting with antibodies to NCAM (Fig. 3 b). Only IC180 pelleted with TGN membranes, whereas IC140 did not.

One of the known binding partners of the intracellular domain of NCAM180 is spectrin (Pollerberg et al., 1986, 1987). At least two spectrin isoforms, spectrin  $\beta$ I and  $\beta$ III, form a meshwork lining Golgi membranes (De Matteis and Morrow, 1998, 2000; Holleran and Holzbaaur, 1998; Lipincott-Schwartz, 1998). In neurons maintained for 1–5 d *in vitro*,  $\alpha$ I $\beta$ I spectrin (hereafter called spectrin) was detected in all neurites, whereas in neurons maintained for 20 d *in vitro*,  $\alpha$ I $\beta$ I spectrin was detected only in dendrites. Spectrin accumulated in varicosities and colocalized with NCAM clusters (Fig. 3 c) that overlapped completely with NCAM180 labeling (unpublished data). Immunoblotting confirmed that the isolated TGN membranes contained  $\beta$ I spectrin, as detected with  $\beta$ I spectrin-specific antibodies (Fig. 3 a) and polyclonal antibodies against  $\alpha$ I $\beta$ I spectrin (Fig. 3 d). We then determined whether the ability of IC180 to bind TGN membranes depended on the presence of non-covalently associated proteins, including the spectrin meshwork, by briefly incubating TGN membranes in alkaline sodium carbonate solution, thereby removing peripheral proteins. After this treatment, spectrin was no longer detectable on TGN membranes (Fig. 3 d). Also, IC180 no longer precipitated with TGN membranes (Fig. 3 b). Because alkaline treatment could have not only removed spectrin from TGN membranes but may also have denatured other TGN membrane-associated binding partners for IC180, TGN membranes were incubated with rabbit polyclonal antibod-

ies to spectrin before assaying for IC180 binding. After this treatment, binding of IC180 was significantly inhibited, indicating that spectrin is a linker molecule that mediates binding of IC180 to TGN membranes (Fig. 3 e). As a control, the immunoglobulin fraction from nonimmune rabbits did not show any inhibition of binding (Fig. 3 e). It is therefore conceivable that NCAM180 at the cell surface interacts with TGN organelles via spectrin.

### Movement of NCAM clusters and associated intracellular organelles

To visualize the distribution and movement of NCAM in association with TGN organelles, two strategies were pursued. Live hippocampal neurons were stained by indirect immunofluorescence using monoclonal antibodies to NCAM under conditions in which antibody-induced cross-linking of primary antibodies was minimized. Alternatively, neurons were transfected with NCAM180 tagged with GFP (NCAM180–GFP). NCAM180–GFP showed a distribution identical to that of immunocytochemically detectable endogenous NCAM180 and “total” cell surface NCAM in that it accumulated in clusters associated with varicosities along neurites and, in particular, also in growth cones (unpublished data). In both cases, intracellular organelles colocalizing with NCAM were observed using DIC optics. We also made use of the possibility to label TGN organelles with the vital styryl fluorescent dyes FM1-43 or FM4-64. Short-term application of these dyes is known to label presynaptic boutons via activity-dependent uptake of dyes into synaptic

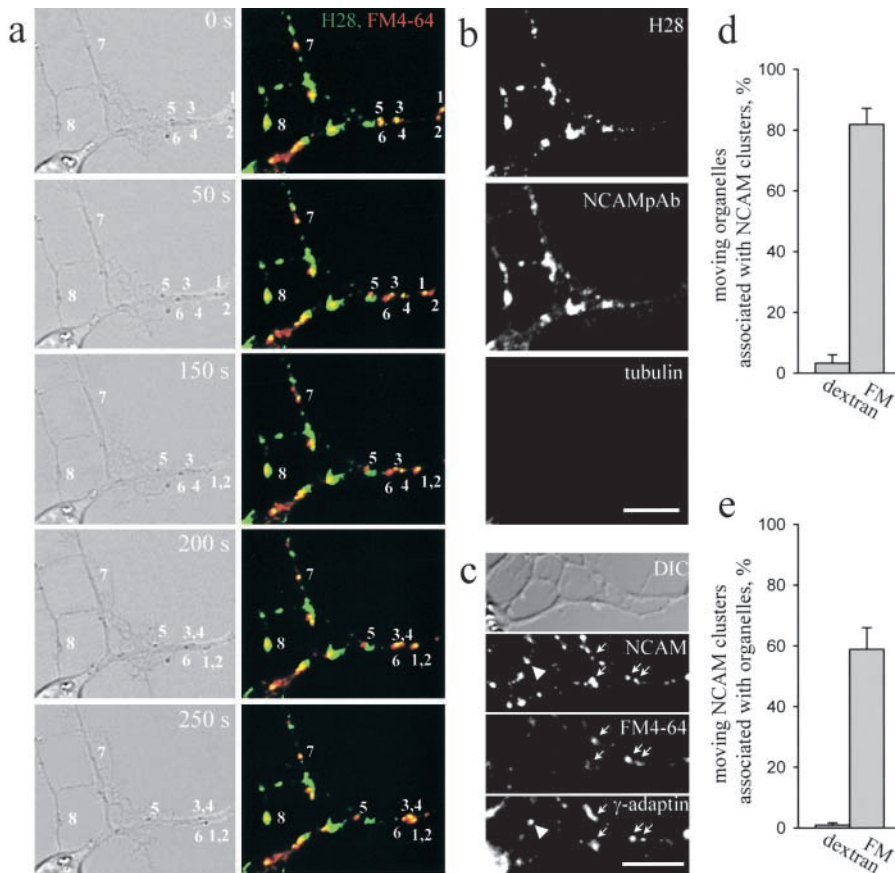


**Figure 4. Movement of NCAM-immunoreactive clusters associated with TGN organelles.** (a) Time-lapse video recording of the movements of NCAM-immunoreactive clusters and associated intracellular organelles along neurites of a hippocampal neuron maintained for 3 d in culture. The neuron was stained by indirect immunofluorescence using monoclonal NCAM antibody (H28, green) applied to live cultures. FM4-64 (red) applied to the culture 24 h before application of the antibody was used to label organelles. NCAM-immunoreactive clusters (marked by 1–8) overlap with intracellular organelles loaded with FM4-64, with the yellow color indicating coincident immunofluorescence signals. Organelles are also seen as dark granules on the corresponding DIC image. Clusters associated with the organelles move along neurites intermittently and bidirectionally. See also Video 1 (available at <http://www.jcb.org/cgi/content/full/jcb.200205098/DC1>). (b) At the end of the video recording, the culture was fixed and stained with NCAM polyclonal antibodies. All clusters revealed by monoclonal NCAM immunostaining (H28) were stained with NCAM polyclonal antibodies (NCAM pAb). Antibodies to tubulin applied together with NCAM polyclonal antibodies to nonpermeabilized culture to monitor

membrane integrity do not show any staining. Bar, 10  $\mu$ m (for a and b). (c) A hippocampal neuron maintained for 3 d in culture was stained with antibodies against NCAM and  $\gamma$ -adaptin. The FM4-64 dye applied to the culture 24 h before application of the antibody was used to label organelles. FM4-64-labeled organelles (arrows) overlap with NCAM clusters and are  $\gamma$ -adaptin positive.  $\gamma$ -Adaptin-positive organelles not labeled with FM4-64 are also seen (triangle). Bar, 10  $\mu$ m. (d) Mean percentage of mobile FM4-64- or RITC-dextran-labeled organelles associated with NCAM clusters. (e) Mean percentage of mobile NCAM clusters associated with FM4-64- or RITC-dextran-labeled organelles. Data present mean  $\pm$  SEM ( $n > 15$  neurons,  $>300$  organelles,  $>500$  NCAM clusters).

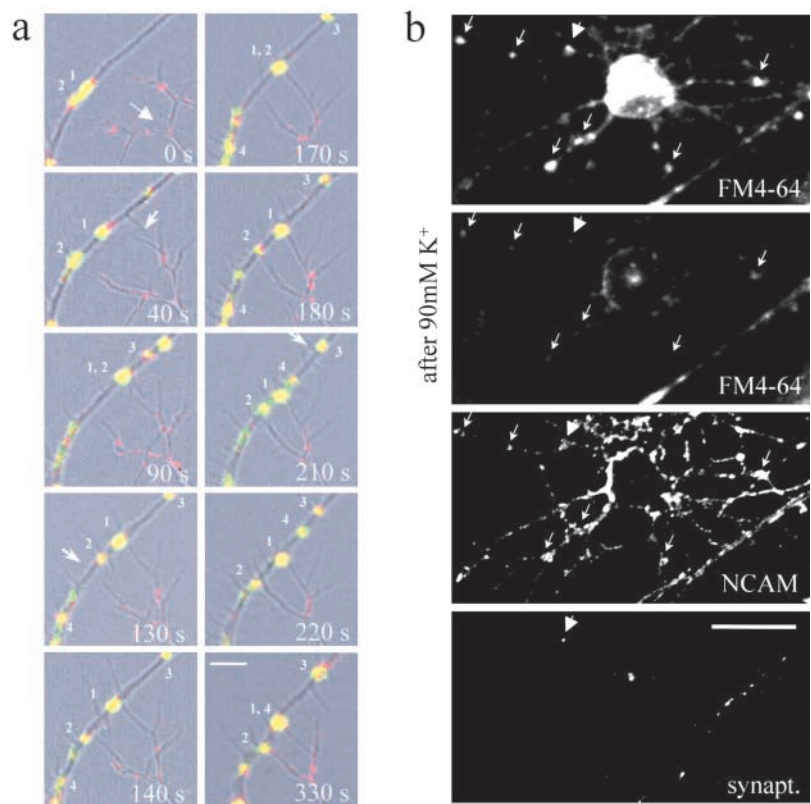
vesicles (Cochilla et al., 1999). However, after prolonged exposure of neurons to these dyes, they label multiple intracellular organelles, mostly TGN or Golgi-like structures (Maletic-Savatic and Malinow, 1998; Maletic-Savatic et al., 1998). Most of the organelles labeled for 24 h with the dyes (80%) coincided with NCAM-immunoreactive and NCAM180-GFP clusters in transfected neurons. Video recordings showed that NCAM-immunoreactive clusters and intracellular organelles moved bidirectionally along neurites (Fig. 4 a; see also Videos 1 and 2, available at <http://www.jcb.org/cgi/content/full/jcb.200205098/DC1>). Analyses of DIC images and FM4-64 fluorescence showed that NCAM clusters were consistently associated with intracellular organelles loaded with FM4-64 during their movement.

To show that NCAM-immunoreactive clusters that moved during the time-lapse recordings were located at the plasma membrane and not endocytosed during image acquisition, neurons were fixed and stained with polyclonal antibodies to NCAM using secondary antibodies carrying a different fluorochrome to distinguish live-labeled from fixed-labeled NCAM. All NCAM-immunoreactive clusters that moved during the time-lapse recording were stained with polyclonal antibodies to NCAM on nonpermeabilized cells,

confirming that they had moved in the plasma membrane rather than in endosomes or other intracellular organelles (Fig. 4 b). Antibodies to tubulin applied in a mixture with NCAM polyclonal antibodies to control for membrane integrity did not give any staining. The same results were obtained when polyclonal antibodies were applied to live neurons at 4°C to block possible endocytosis (unpublished data), confirming surface location of NCAM-immunoreactive clusters. Also, staining of NCAM180-GFP-transfected nonpermeabilized neurons with polyclonal antibodies to NCAM showed that NCAM180-GFP clusters were located at the cell surface (unpublished data). To further confirm that organelles loaded with FM4-64 were TGN organelles, we acquired images of the hippocampal neurons loaded with FM4-64 and subsequently labeled the neurons with antibodies to  $\gamma$ -adaptin: the majority of FM4-64-loaded organelles (89%,  $n = 162$ ) were  $\gamma$ -adaptin positive (Fig. 4 c). Approximately 10% of  $\gamma$ -adaptin-positive organelles were not loaded with FM4-64, probably due to the limited time of incubation with FM4-64.

Autophagic vacuoles constitute another class of large vesicles that can be observed in axons (Hollenbeck, 1993; Overly et al., 1996). To test whether NCAM clusters move in association

**Figure 5. Accumulation of NCAM-immunoreactive clusters and associated organelles at the contact site between two neurites.** Hippocampal neurons maintained for 3 d in culture were stained with monoclonal NCAM antibodies (red). Intracellular organelles were loaded with FM1-43, applied for 24 h before the start of recording (green). Immediately at the start of recording, the growth cones of the neurite extending from the lower right hand corner (arrow) have not reached the neighboring target neurite. NCAM-immunoreactive clusters associated with intracellular organelles marked with FM1-43 and seen in yellow (marked by 1–4) move along the target neurite. During recording three contacts were formed. At the end of the recording, each contact was associated with an NCAM-immunoreactive cluster and intracellular organelles on the target neurite. Bar, 10  $\mu$ m. See also Video 3 (available at <http://www.jcb.org/cgi/content/full/jcb.200205098/DC1>). (b) Hippocampal neuron maintained for 4 d in culture was stimulated with a solution containing 90 mM  $K^+$ . Intracellular organelles were loaded with FM4-64, applied for 24 h before stimulation. Stimulation induced destaining of FM4-64-labeled organelles (arrows). The neuron was fixed and stained with antibodies against NCAM and synaptophysin. The staining shows that FM4-64-labeled organelles coincide with NCAM clusters. Most of the organelles were synaptophysin immunonegative. Triangle arrow points to the organelle that was colocalized with synaptophysin accumulation. Bar, 20  $\mu$ m.



with these organelles, we labeled them with RITC-dextran, which has been shown to accumulate in these organelles when applied to the culture medium for several hours (Hollenbeck, 1993). After loading with RITC-dextran, live hippocampal neurons were labeled with NCAM antibodies. Time-lapse analysis showed that NCAM clusters were very rarely associated with RITC-dextran-labeled organelles (<5%) and moved independently of them (Fig. 4, d and e).

#### NCAM clusters and associated intracellular organelles accumulate at sites of neurite-to-neurite contacts

Hippocampal neurons maintained for 2–3 d in culture formed multiple intercellular contacts. These contacts were intensely stained for NCAM and often contained intracellular organelles. To study the movement of NCAM clusters and associated intracellular organelles during contact formation, we visualized NCAM distribution by indirect immunofluorescence and recorded a time series of movements of NCAM-immunoreactive clusters during contact formation between hippocampal neurons.

Fig. 5 shows the formation of three contacts between filopodia of a neurite approaching the central part of the target neurite (see also Video 3, available at <http://www.jcb.org/cgi/content/full/jcb.200205098/DC1>). The organelles were loaded with FM1-43 for 24 h before application of NCAM monoclonal antibody. Prior to contact formation, NCAM-immunoreactive clusters moved bidirectionally along the neurite in association with FM1-43-positive intracellular organelles (Fig. 5). Growth cones approaching neurites were often not labeled by NCAM antibodies, probably due to the fact that the growth cones were formed

after the antibody was applied (usually >20 min after antibody labeling). After establishment of physical contacts between the growth cone and the target neurite (Fig. 5 a, 40 s), NCAM-immunoreactive clusters and associated organelles that had moved along the target neurite started to accumulate at the site of contact (Fig. 5 a, 90 s, cluster No. 1). The clusters and associated intracellular aggregates often passed several times through the actual site of contact, but finally one or several clusters and associated organelles were “trapped” at the contact site and remained there until the end of the recordings (10–100 min). After the initial contact, neurites formed a “varicosity” or “bouton,” probably representing the site where apposing membranes approach each other. Organelles were trapped within this thickening that was in close proximity to the intersection point between neurites, but did not always exactly coincide with the intersection point between neurites (Fig. 5, organelles 1 and 2). Sometimes, the growth cone contacted the target neurite at the site of an NCAM-immunoreactive cluster. In this case, the NCAM-immunoreactive cluster and associated intracellular aggregates remained at the site of contact from the moment of its formation. Out of 14 contacts recorded, 4 contacts were formed at the sites where NCAM-immunoreactive clusters and intracellular organelles were already present, whereas 10 of the 14 contacts were initially formed at NCAM-immunonegative sites in the organelle-free areas of neurites.

#### FM4-64-loaded TGN organelles are capable of exocytosis

TGN-derived organelles are the major carriers between the TGN and plasma membranes (Nakata et al., 1998; Toomre

et al., 1999, 2000; Polishchuk et al., 2000), being capable of fusing with the plasma membrane. To show that TGN organelles loaded with FM4-64 undergo exocytosis in response to external stimuli, we stimulated neurons with 90 mM  $K^+$ . In agreement with previous observations on exocytosis of axonal synaptic precursor organelles (Matteoli et al., 1992; Kraszewski et al., 1995; Dai and Peng, 1996; Zakharenko et al., 1999) and dendritic and somatic TGN organelles (Maletic-Savatic and Malinow, 1998; Maletic-Savatic et al., 1998), this stimulation induced destaining of the FM4-64-labeled organelles in neurites and soma, demonstrating their fusion with the plasma membrane (Fig. 5 b). Exocytosis was observed not only for axonal but also for dendritic organelles, as shown by the absence of synaptophysin immunostaining on most of the processes that display FM dye-labeled organelles (Fig. 5 b). Evoked exocytosis in somatic and dendritic compartments was observed in our experiments starting already from day four in culture, which is earlier than observed by Maletic-Savatic and Malinow (1998). The reason for this could be that hippocampal neurons in our experiments were obtained from postnatal mice and maintained in serum-containing medium, whereas neurons used by Maletic-Savatic and Malinow (1998) were derived from embryonic rat brains and maintained in serum-free medium.

#### Accumulation of NCAM at sites of contact accompanies synaptic differentiation of initial contacts

To show that accumulation of NCAM accompanies synaptic differentiation of the initial contact, cultures were stained by short-term application of FM4-64 in a solution containing 90 mM  $K^+$  according to a protocol that is accepted to stain functional synapses (Ryan et al., 1993; Liu and Tsien, 1995). The loading of synapses with FM4-64 was performed three times with a 1-h interval between loadings to allow for the detection of contacts *de novo* undergoing activity-stimulated endocytosis during this time interval. Because recycling synaptic vesicles and synapse-specific proteins can be found distributed along neurites without any evident contacts (Matteoli et al., 1992; Kraszewski et al., 1995; Dai and Peng, 1996; Rao et al., 1998; Zakharenko et al., 1999; Ahmari et al., 2000), we identified differentiating contacts as contacts between neurites visualized by DIC optics and labeled by acute application of an FM4-64 dye in response to  $K^+$  stimulation (Fig. 6). Fig. 6 a shows an NCAM180-GFP-transfected neuron and a few synapses distributed along neurites that had been loaded with FM4-64. The second and third loading with FM4-64 (Fig. 6, b and c) at 60 and 120 min afterwards revealed several new endocytosis-competent contacts that had formed during this time period. These events occurred at sites of NCAM180-GFP accumulation (Fig. 6 d). To further show that these contacts are exocytosis competent, we stimulated synaptic activity by application of 90 mM  $K^+$  for 1 min (Fig. 6 e). This treatment led to complete destaining of the newly labeled contacts, confirming that they were functionally active. Neurons were then fixed and stained with antibodies to synaptophysin (Fig. 6 f), confirming that the observed FM4-64-labeled contacts had accumulated synaptic vesicles and thus likely represent nascent synapses. FM4-64-nega-

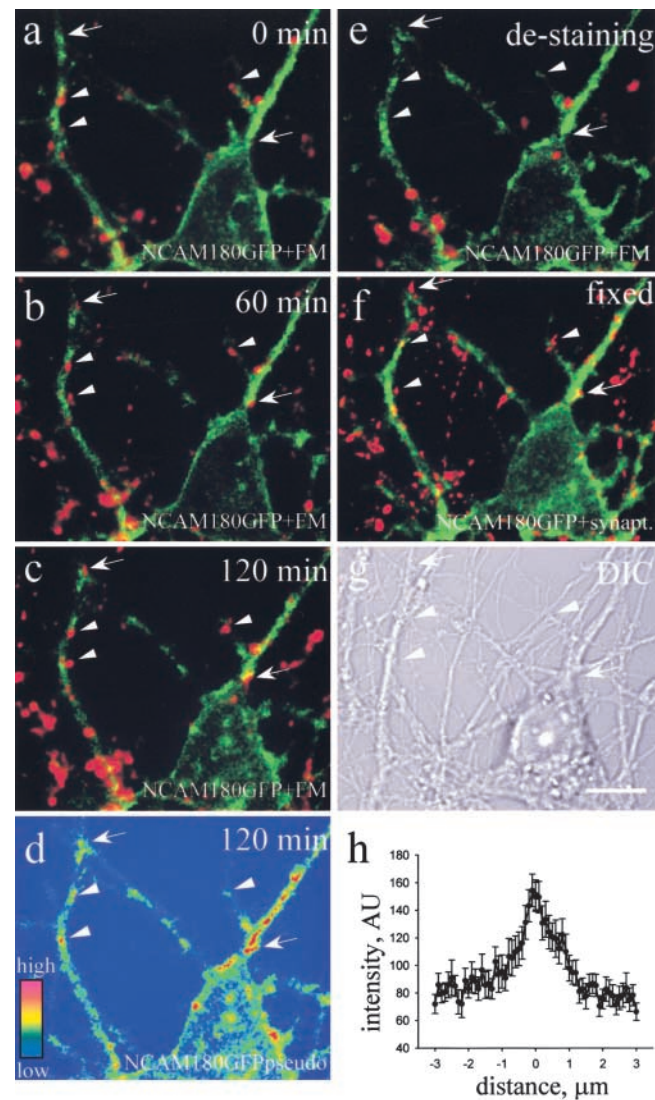


**Figure 6. Sites of NCAM180-GFP accumulation become functional contacts.** NCAM180-GFP-transfected neurons were maintained for 5 d in culture. (a–c) Synapses were stained three times with a 1-h interval between a, b, and c by acute application of FM4-64 (red) in a solution containing 90 mM  $K^+$ . Within 2 h, several new sites undergoing depolarization-induced endocytosis of FM4-64 were found (arrows). Pseudocolored picture of NCAM180-GFP (red and yellow colors correspond to the higher density of NCAM180-GFP) shows that synaptic differentiation occurs at sites of NCAM180-GFP accumulation (d). Pre-existing functional contacts (arrowheads) also colocalize with NCAM180-GFP accumulations. Synapses were destained by application of the medium containing 90 mM  $K^+$  without FM4-64 (e). The staining with antibodies against synaptophysin confirmed that FM4-64-stained synaptic boutons coincided with synaptophysin accumulations (f). (g) Corresponding DIC image. (h) Average profile of NCAM180-GFP distribution along neurites in the vicinity of contact sites. Zero coordinate (distance axis) corresponds to the point apposed to acutely FM4-64-loaded boutons. Bar, 10  $\mu m$ .

tive and synaptophysin-positive puncta probably represent functionally immature synapses or transport packages moving along axons (Ahmari et al., 2000). Altogether, we recorded 29 cases of synaptic differentiation. Only three cases were detected at contact sites without accumulation of

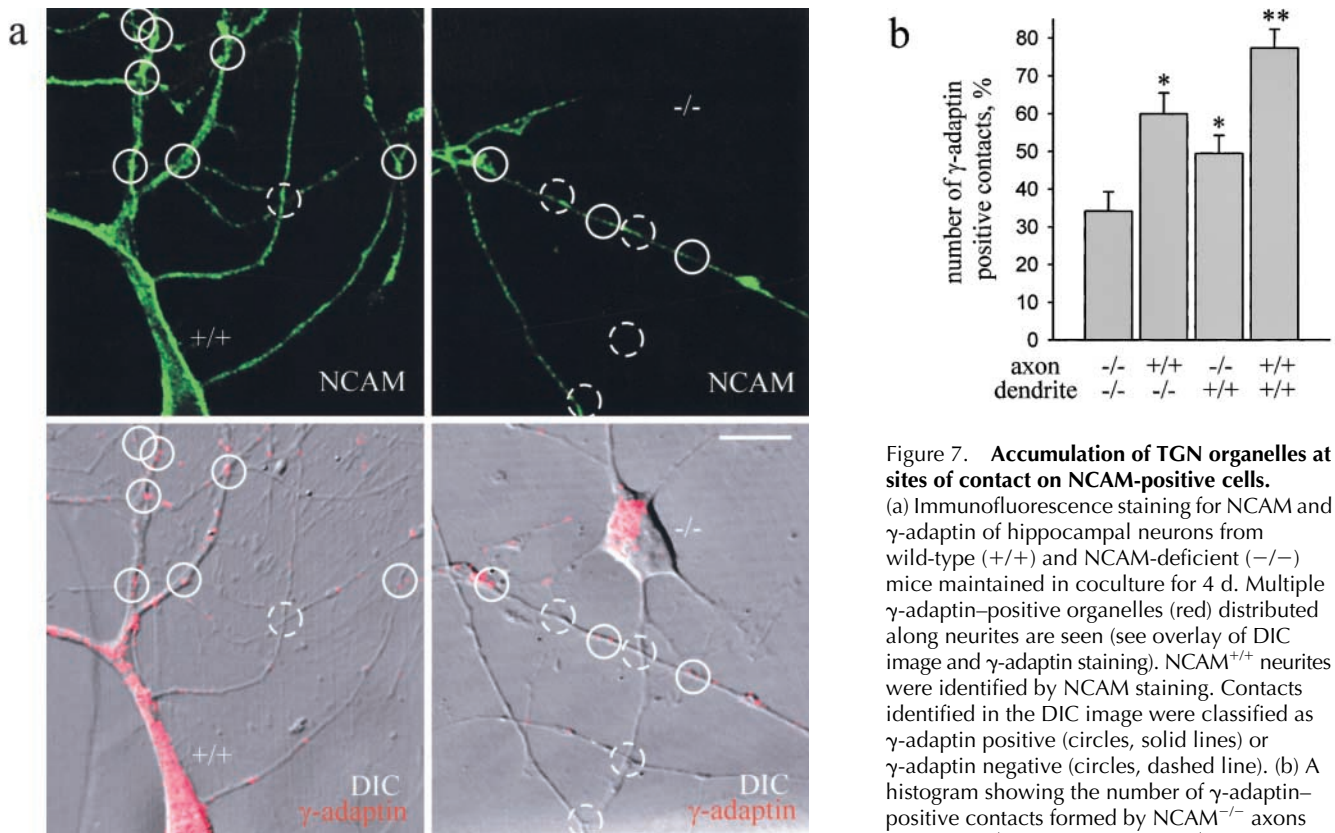


**Figure 7. Accumulation of TGN organelles at sites of contact on NCAM-positive cells.**

(a) Immunofluorescence staining for NCAM and  $\gamma$ -adaptin of hippocampal neurons from wild-type (+/+) and NCAM-deficient (-/-) mice maintained in coculture for 4 d. Multiple  $\gamma$ -adaptin-positive organelles (red) distributed along neurites are seen (see overlay of DIC image and  $\gamma$ -adaptin staining). NCAM<sup>+/+</sup> neurites were identified by NCAM staining. Contacts identified in the DIC image were classified as  $\gamma$ -adaptin positive (circles, solid lines) or  $\gamma$ -adaptin negative (circles, dashed line). (b) A histogram showing the number of  $\gamma$ -adaptin-positive contacts formed by NCAM<sup>-/-</sup> axons on NCAM<sup>-/-</sup> dendrites, NCAM<sup>+/+</sup> axons on NCAM<sup>-/-</sup> dendrites, NCAM<sup>-/-</sup> axons on

NCAM<sup>+/+</sup> dendrites, and NCAM<sup>+/+</sup> axons on NCAM<sup>+/+</sup> dendrites as percentage of the total number of all contacts analyzed. Data present mean  $\pm$  SEM (six cultures, two independent experiments). \* $P < 0.01$ , paired  $t$  test shows a significant difference in the percentage of  $\gamma$ -adaptin-positive contacts between NCAM-negative and other types of contacts. Bar, 10  $\mu$ m.

NCAM180-GFP, whereas 26 nascent synapses coincided with NCAM180-GFP clusters. The average profile of NCAM180-GFP distribution along neurites showed a peak that was apposed to FM4-64-loaded synapses (Fig. 6 h). Interestingly, two of the three nascent synapses that were formed at contact sites without NCAM180-GFP accumulation were not stained with FM4-64 within 1 h after their appearance, suggesting that they were not stabilized. In contrast, only one of the recorded 26 nascent synapses coinciding with NCAM180-GFP clusters was not stabilized. These results indicate that accumulation and stabilization of intracellular organelles coupled to clusters of NCAM180-GFP accompany synaptic differentiation and suggest that NCAM is important for the stabilization of nascent synapses.

#### NCAM promotes stabilization of TGN organelles at sites of contact

To investigate whether NCAM plays a role in the stabilization of organelles at sites of contact, we used heterotypic cocultures of hippocampal neurons derived from wild-type and NCAM-deficient mice (Fig. 7). As shown previously, wild-type neurons maintained for 9 d in vitro had significantly more synaptic contacts than neurons from NCAM-deficient mice (Dityatev et al., 2000). We defined a contact as an intersection point between two neurites on the DIC image with an intersection angle of  $>10^\circ$ . In cultures

maintained for 4 d in vitro,  $\gamma$ -adaptin-immunoreactive TGN organelles were also significantly more often associated with contact sites between heterotypic axons and dendrites ( $\sim 55\%$  of contacts) when compared with NCAM-negative contacts (35% of contacts), showing that heterophilic interactions of NCAM become apparent in a choice situation. TGN organelles were even more often associated with sites of contact formed by NCAM-positive axons and NCAM-positive dendrites ( $\sim 80\%$ ), implicating a possible contribution of homophilic interactions.

To further investigate the mechanism of TGN organelle stabilization by NCAM, we analyzed contact formation and organelle accumulation at contact sites in homotypic cultures of hippocampal neurons from wild-type or NCAM-deficient mice (Fig. 8). We identified the accumulation of organelles as a persistent association of organelles with the contact until the end of recordings. In cultures of neurons from NCAM-deficient mice, the number of newly formed contacts with accumulated organelles was reduced when compared with cultures from wild-type mice. Whereas 20 of 24 contacts between wild-type neurons accumulated organelles 1–15 min after initial contact formation, NCAM-deficient neurons accumulated organelles at contact sites in only 3 of 18 cases ( $P < 0.001$ , chi-square test). The decreased capability to accumulate organelles at sites of contact in NCAM-deficient neurons could be due to the reduced time of contact.



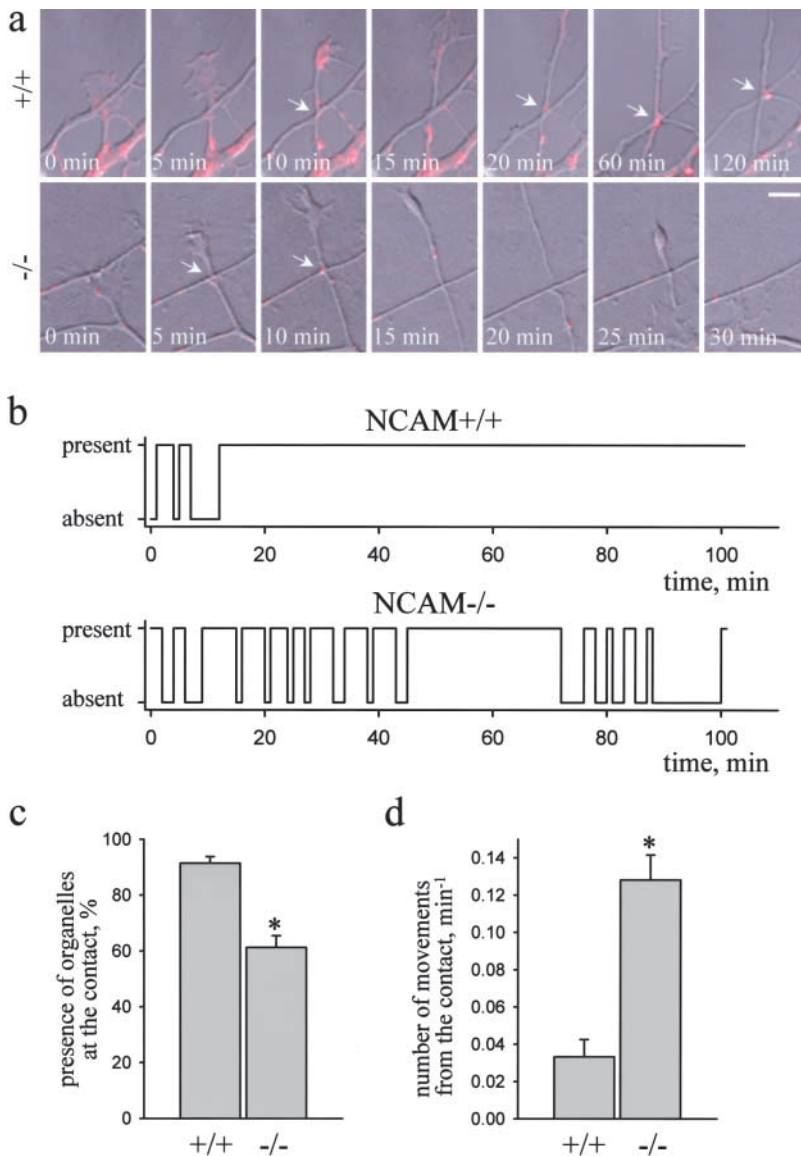


**Figure 8. NCAM stabilizes TGN organelles at sites of contact.** (a) Contact formation between NCAM<sup>+/+</sup> and NCAM<sup>-/-</sup> neurons. TGN organelles were labeled with FM4-64 applied for 24 h (“prolonged” protocol). Organelles were trapped at the contact between NCAM<sup>+/+</sup> neurons 20 min after contact formation and remained associated with the contact for 100 min until the end of recordings. Organelles were not trapped at the contact between NCAM<sup>-/-</sup> neurons, appearing only transiently at the site of contact (see 10 min) (arrows). The contacting neurite was retracted 30 min after contact formation. Bar, 5  $\mu$ m. (b) Representative diagrams showing the dynamics of TGN organelle accumulation at the site of contact recorded in NCAM<sup>+/+</sup> and NCAM<sup>-/-</sup> cultures. Note the continuous presence of organelles at contacts between NCAM<sup>+/+</sup> neurons (trapping event). (c) Histogram showing the mean time that a contact contained organelles as a percentage of the total recording time (set to 100%). (d) Histogram showing the mean number of events when organelles moved away from the contact. \* $P < 0.001$ ,  $t$  test shows a significant difference between NCAM-deficient and wild-type neurons.

Contacts between NCAM-deficient neurons were more often disrupted due to retraction of neurites when compared with wild-type neurons (10 of 18 newly formed contacts in NCAM-deficient neurons underwent retractions within 5–20 min after contact formation, but only 1 of 24 in wild-type neurons,  $P < 0.001$ , chi-square test) (Fig. 8 a). These retractions were not accompanied by any signs of damage to neurites and were often followed by regrowth of the retracted neurites in the previous direction. To determine more precisely the role of NCAM in the anchoring of organelles at sites of contact, we estimated the time that organelles spent at contact sites and the persistence of their association with the contact. The time that contacts contained organelles in NCAM-deficient neurons was  $\sim 60\%$  of the total recording time, being  $\sim 30\%$  less when compared with wild-type neurons (90% of the total recording time). Moreover, organelles moved away from the contacts approximately four times more often in NCAM-deficient neurons when compared with wild-type neurons (Fig. 8). We conclude that NCAM is important

both for stabilization of initial contacts and for stabilization of organelles at sites of contact.

## Discussion

We show in this study that NCAM mediates accumulation of TGN organelles at sites of cell-to-cell contact. TGN organelles that can form large pleiomorphic structures up to several microns in diameter mediate the majority of cargo transport from the Golgi network to the plasma membrane (Nakata et al., 1998; Toomre et al., 1999, 2000; Polishchuk et al., 2000; Stephens and Pepperkok, 2001). To label TGN organelles in live cells we used the styryl dyes FM1-43 or FM4-64. These dyes have been shown to accumulate in the Golgi or Golgi-like structures after prolonged ( $>8$  h) incubation time (Maletic-Savatic and Malinow, 1998; Tarabal et al., 2001). To prove this, Maletic-Savatic and Malinow (1998) correlated the distribution of FM1-43-labeled organelles with NBD C6-ceramide, which localizes to the TGN. Moreover, the combined fluorescence and electron

microscopic analyses show that FM1-43-labeled organelles correspond to the TGN. In agreement with our data, only a small proportion of the FM1-43-loaded organelles were identified as endosomes or lysosomes (Maletic-Savatic and Malinow, 1998). The reason for this is that FM dyes reside in endosomal compartments only very transiently before being transferred to TGN-like structures. This view is supported by data showing that the trans-Golgi network interacts with the recycling endosomal system (Mallard et al., 1998) and that TGN-associated proteins, such as TGN-38, could be found in endosomes (Nakata et al., 1998). Recycling of the mannose-6-phosphate receptor from late endosomes to the TGN is also well characterized (Clague, 1998).

TGN organelles are responsible for the trafficking of a variety of newly synthesized proteins, including synapse-specific proteins such as synaptophysin and SNAP-25 (Nakata et al., 1998). They are involved in the constitutive and regulated trafficking pathways both in dendrites and axons (Maletic-Savatic and Malinow, 1998; Nakata et al., 1998). Being stabilized in the vicinity of a contact between an axon and dendrite, these organelles provide the proteins necessary for further synaptic differentiation.

The time course of accumulation of synaptic precursor organelles and different synaptic proteins at sites of contact and the molecular mechanisms underlying post- and presynaptic differentiation have been well studied in recent years (Burry, 1986, 1991; Dai and Peng, 1996; Mammen et al., 1997; Rao et al., 1998; Ahmari et al., 2000; Friedman et al., 2000; Lee and Sheng, 2000; Scheiffele et al., 2000; Zhai et al., 2001). We show that NCAM is one of the initial proteins that accumulates at sites of contact within several minutes after contact formation. Our study is the first, to our knowledge, showing that recognition molecules, such as NCAM, provide a direct link between extracellular cues and intracellular organelles to stabilize them at nascent synapses. This finding fits well with recent data on the involvement of NCAM in the mobilization and cycling of synaptic vesicles at the neuromuscular junction (Polo-Parada et al., 2001). The first step in this process is the formation of a complex between clusters of NCAM and TGN organelles before neurites contact each other (Fig. 9). It is therefore noteworthy that organelle-rich varicosities have also been described in the intact tissue (Fiala et al., 1998; Shepherd and Harris, 1998). The complex between NCAM and intracellular organelles is generally formed outside of the initial contact. Because organelles are driven by intracellular motors, we infer that the mobility of NCAM clusters depends on these.

The link between organelles and cell surface-integrated NCAM180 requires the involvement of peripheral proteins associated with the membrane of the TGN organelle. Here, we show that spectrin is one of these molecules, underscoring a putative mechanism for recent findings in *Drosophila* on the importance of spectrin in accumulation of synaptic proteins and synaptic transmission (Featherstone et al., 2001). Spectrin has been shown to bind to NCAM180, the largest major isoform of NCAM, but does not bind to NCAM140 (Pollerberg et al., 1986, 1987). Spectrin is highly enriched in neurite varicosities containing vesicular and tubular membranous compartments (Koenig et al., 1985), and the cytoplasmic surface of a variety of intracel-

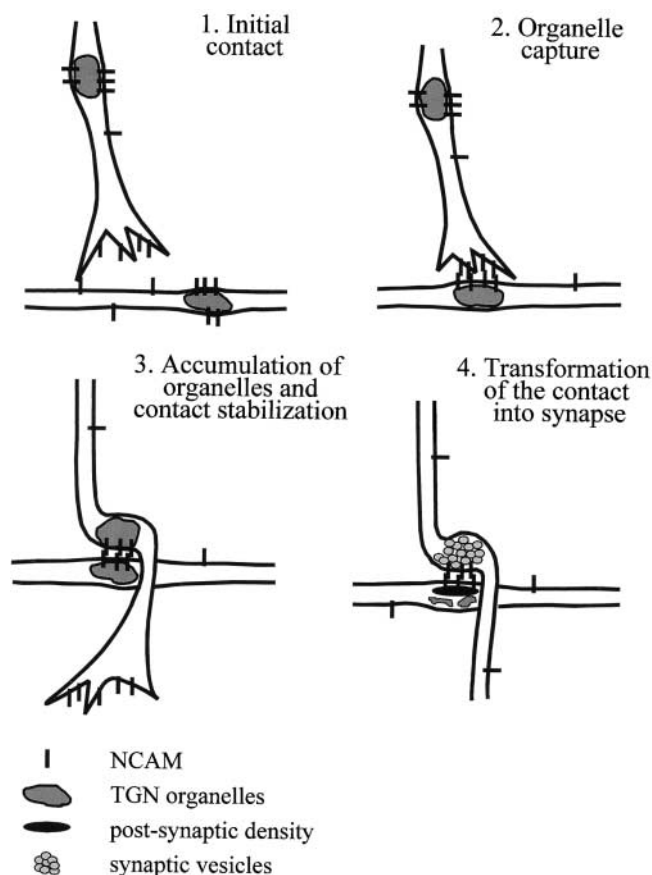


Figure 9. A model of NCAM-mediated accumulation of TGN organelles at sites of contact followed by synaptic differentiation.

lular organelles is lined with the spectrin-actin cytoskeleton (De Matteis and Morrow, 1998; Holleran and Holzbaur, 1998; Lippincott-Schwartz, 1998). Spectrin is also tightly colocalized both with TGN organelles and NCAM clusters and mediates binding of the intracellular domain of NCAM180, but not NCAM140, with TGN organelles, in agreement with the experiments by Pollerberg et al. (1986, 1987), which were performed under completely different conditions. It is conceivable that membrane phospholipids are also involved in this interaction (Haest et al., 1978; Sikorski and Kuczek, 1985; McKiernan et al., 1997).

That NCAM indeed mediates the stabilization of initially formed contacts between neurites is underscored by the observation that in heterogenotypic cocultures, contacts on NCAM-deficient neurons resulted in a reduction of synaptic coverage (Dityatev et al., 2000). Data presented in this paper provide further insights into the mechanisms of contact formation, showing that trapping of NCAM-associated TGN organelles represents an early event in synaptogenesis that entails stabilization of contacts. This stabilization could be shown in our study to result in the transformation of the initial contacts into functional contacts undergoing exo- and endocytosis of synaptic vesicles. Analysis of TGN organelle accumulations in heterogenotypic cultures suggests that heterophilic and homophilic interactions align the TGN at sites of contact. Interestingly, in our previous study (Dityatev et al., 2000), heterophilic interactions also appeared to be im-

portant for neurons maintained for 7 d in vitro. In the present study, neurons maintained for 3–4 d in vitro were analyzed, i.e., at stages when the first contacts are formed. The interesting difference between the two studies is that at later developmental stages, only postsynaptically localized NCAM appears to be important for stabilization. These observations imply that in addition to the primary stabilization in the presence of NCAM either pre- or postsynaptically, there may be secondary selection processes, which destabilize synapses expressing NCAM presynaptically, but not postsynaptically. Interestingly, NCAM does not appear to be the only player in the secondary stabilization process, as in homogenotypic cultures comprising only NCAM-deficient neurons, synaptic coverage is as efficient as in cultures containing wild-type neurons (Dityatev et al., 2000). Thus, in a choice situation, NCAM is most likely a preferred candidate for the stabilization of contacts between cells. However, the present study also shows that NCAM may not be the only molecule involved in the stabilization of initial contacts and accumulation of TGN organelles at these contacts, which are transformed into functional synaptic machinery. It is therefore likely that other molecular mechanisms could contribute to the anchoring of intracellular organelles to sites of initial cell contact and thus contribute to the transformation of the nascent synapse to the mature, functionally active synapse.

## Materials and methods

### Antibodies and toxins

Rabbit polyclonal antibodies (Martini and Schachner, 1986) and rat monoclonal antibody H28 against mouse NCAM recognizing extracellular epitopes of the protein (Gennarini et al., 1984) were generated as previously described. We also used mouse monoclonal antibodies against  $\gamma$ -adaplin and EEA1 (Transduction Laboratories), rabbit polyclonal antibodies against Rab4 and goat polyclonal antibodies against  $\beta$ I spectrin (Santa Cruz Biotechnology, Inc.), rat monoclonal antibody against lamp-1, mouse monoclonal antibody against tubulin and mouse monoclonal antibody 5B8 against NCAM (Developmental Studies Hybridoma Bank, Iowa City, IA), rabbit polyclonal antibodies against erythrocyte spectrin, mouse monoclonal antibodies against  $\beta$ -COP, rabbit nonimmune immunoglobulins (Sigma-Aldrich), and secondary antibodies against goat, rabbit, rat, and mouse Ig coupled to HRP, Cy2, Cy3, or Cy5 (Dianova). DL-AP5 and 6-cyano-7-nitroquinoxaline-2,3-dione (CNQX) were purchased from Tocris.

### Cultures of hippocampal neurons

Cultures of hippocampal neurons were prepared from 1- to 3-d-old C57BL/6J mice (Dityatev et al., 2000) and maintained on glass coverslips in hormonally supplemented culture medium containing 10% of specifically tested horse serum (Sigma-Aldrich). Coverslips were coated overnight with poly-L-lysine (100  $\mu$ g/ml) in conjunction with laminin (20  $\mu$ g/ml). For time-lapse video recordings, cells were maintained in Corning dishes (35 mm in diameter) with a glass bottom (MatTek Corporation). Dishes were sealed in the incubator with parafilm and transferred to the heating stage of the confocal laser scanning microscope for recording at 35°C.

### Indirect immunofluorescence staining

Indirect immunofluorescence staining of fixed cells was performed as previously described (Dityatev et al., 2000). Antibodies to NCAM were applied to fixed nonpermeabilized cells for 30 min at room temperature and detected with fluorochrome-coupled secondary antibodies applied for 30 min at room temperature. Antibodies against  $\gamma$ -adaplin,  $\beta$ -COP, synaptophysin, EEA1, Rab4, lamp-1, spectrin, or tubulin were applied after permeabilization of cells with 0.25% Triton X-100 for 60 min at room temperature and detected with corresponding secondary antibodies. In experiments aimed to monitor membrane integrity, the permeabilization step was omitted. Images were acquired using a confocal laser scanning microscope LSM510 (ZEISS). For indirect immunofluorescence staining of

live cultures, monoclonal NCAM antibody was applied in culture medium to live cultures for 15 min and detected with fluorochrome-coupled secondary antibodies applied for 5 min, all in a CO<sub>2</sub> incubator. To minimize antibody-induced cross-linking of NCAM in live cells, different concentrations of primary and secondary antibodies were tested to select the concentrations resulting in a staining pattern similar to that obtained after fixation of cells with paraformaldehyde.

### Fluorescence labeling of intracellular organelles

The fluorescent dyes FM1-43 or FM4-64 (Molecular Probes) were used to label intracellular organelles mainly of TGN origin (Maletic-Savatic and Malinow, 1998). To label autophagic vacuoles, RITC-dextran (Sigma-Aldrich) was used (Hollenbeck, 1993). Cultures were incubated for 24 h in a CO<sub>2</sub> incubator in culture medium containing 10  $\mu$ M FM1-43 or FM4-64, or 1 mg/ml RITC-dextran, and briefly washed four times in culture medium preheated to 37°C. In double labeling experiments, images of FM-stained structures were acquired before the permeabilization step that resulted in washout of the dye.

### Colocalization analysis

A membrane area of 0.4–2  $\mu$ m in diameter with a level of NCAM immunofluorescence intensity that was at least more than two times higher than that of adjacent membranes was identified as an NCAM cluster. An NCAM cluster was considered as overlapping with an organelle when >30% of the cluster area overlapped with the corresponding organelle marker.

### Cell surface staining with Dil

Cells were fixed for 15 min at room temperature with PBS containing 4% paraformaldehyde and washed four times, 5 min each, in PBS. The lipophilic dye Dil (Molecular Probes) was dissolved in sesame oil (Sigma-Aldrich) to saturation (Papa et al., 1995). A drop of this Dil solution (5–10  $\mu$ m in diameter) was applied through the glass pipette onto the soma of the neuron to be labeled. The dye was allowed to spread over the surface of the neuron for 30 min at room temperature before confocal microscopic imaging.

### Labeling of synapses by short-term FM4-64 loading

Cultures were exposed to 15  $\mu$ M FM4-64 in a stimulating solution containing 31.5 mM NaCl, 90 mM KCl, 5 mM Hepes, 1 mM MgCl<sub>2</sub>, 2 mM CaCl<sub>2</sub>, and 30 mM glucose for 1 min in a CO<sub>2</sub> incubator (Ryan et al., 1993; Liu and Tsien, 1995). Washing and imaging of neurons was performed in culture medium containing 10  $\mu$ M 6-cyano-7-nitroquinoxaline-2,3-dione (CNQX) and 50  $\mu$ M DL-AP5 to block synaptic transmission and thus avoid destaining of the synapses. To show that synapses are capable of active exocytosis, they were destained by incubation of cultures in stimulating solution without FM4-64 for 1 min in a CO<sub>2</sub> incubator.

### Production of intracellular domains of NCAM140 and NCAM180

The BamHI sites were introduced at the 5' and 3' ends of the cDNAs encoding the NCAM140 or NCAM180 intracellular domains and were cloned in frame into the BamHI site of pQE30 (QIAGEN). Proteins were expressed in *Escherichia coli* strain M15 and purified on Ni-NTA-agarose (QIAGEN) according to the manufacturer's instructions.

### Construction of the NCAM180–GFP chimera

The NCAM-EGFP chimera was constructed by introducing Ehel sites at the 5' and 3' ends of the coding sequence of the EGFP cDNA (CLONTECH Laboratories, Inc.) using standard PCR technique. EGFP was cloned into the unique Ehel site (position 2133) of an EcoRI-XhoI subfragment of NCAM180. PCR amplification of EGFP and direction of the EGFP insertion were verified by sequencing. The EcoRI-XhoI subfragment was cloned into the pCDNA3 vector, which contained the 5' HindIII-EcoRI fragment of NCAM180.

### Transfection of hippocampal neurons

Cells were transfected 24 h after seeding by the calcium phosphate method (Ethell and Yamaguchi, 1999) using the mammalian transfection kit (Stratagene).

### Gel electrophoresis and immunoblotting

Proteins were separated by 8% SDS-PAGE and electroblotted to nitrocellulose transfer membrane (PROTRAN; Schleicher & Schuell) for 3 h at 250 mA. Immunoblots were incubated with appropriate primary antibodies followed by incubation with peroxidase-labeled secondary antibodies and visualized using Super Signal West Pico reagents (Pierce Chemical Co.) on

BIOMAX film (Sigma-Aldrich). Molecular weight markers were prestained protein standards from Bio-Rad Laboratories or Life Technologies.

### Isolation of TGN membranes

Trans-Golgi membranes were isolated from the brains of 3-mo-old NCAM-deficient mice (Cremer et al., 1994) as previously described (Fath et al., 1997). TGN membranes were resuspended in PEMS (10 mM Pipes, pH 7.0, 1 mM EGTA, 2 mM MgCl<sub>2</sub>, and 0.25 mM sucrose) containing complete EDTA-free protease inhibitor cocktail (Roche).

### Binding of NCAM140 and NCAM180 intracellular domains to TGN membranes

TGN membranes or TGN membranes extracted on ice for 30 min in 0.1 M Na<sub>2</sub>CO<sub>3</sub>, pH 11.5, were used. The extracted TGN membranes were collected by centrifugation through a 0.5 M sucrose-PKM (100 mM potassium phosphate, 5 mM MgCl<sub>2</sub>, 3 mM KCl, pH 6.5) cushion at 259,000 *g*<sub>max</sub> for 30 min at 4°C. Pellets were resuspended in PEMS and washed three times. Intracellular domains of NCAM180 and NCAM140 were added to TGN membranes at a concentration of 40 μg/ml and incubated for 30 min at room temperature. To monitor whether TGN membranes bind to the intracellular domain of NCAM180 via spectrin, TGN membranes were incubated with antibodies to erythrocyte spectrin (50 μg/ml) or nonimmune immunoglobulins (100 μg/ml) as a control for 60 min at room temperature. After incubation, the TGN membranes were collected by centrifugation through a 0.5 M sucrose-PKM cushion at 259,000 *g*<sub>max</sub> for 30 min at 4°C. Pellets were resuspended in PEMS buffer, washed three times, and analyzed by immunoblotting.

### Online supplemental material

The supplementary videos (available online at <http://www.jcb.org/cgi/content/full/jcb.200205098/DC1>) show movement of NCAM-immunoreactive clusters associated with FM4-64-labeled organelles (Video 1), movement of NCAM180-GFP clusters in transfected hippocampal neurons (Video 2), and trapping of NCAM-immunoreactive clusters and associated TGN organelles at sites of interneuronal contacts (Video 3).

We thank Drs. Catherina Becker, Carlos Dotti, Michael Sheetz, and Kai Simons for helpful suggestions. The antibodies against lamp-1 and β-tubulin were obtained from the Developmental Studies Hybridoma Bank under the auspices of the National Institute of Child Health and Human Development.

This work was supported in part by the Deutsche Forschungsgemeinschaft (DI 702/1-1 to A. Dityatev) and a European Molecular Biology Organization short-term fellowship (to V. Sytnyk).

Submitted: 20 May 2002

Revised: 24 September 2002

Accepted: 14 October 2002

## References

- Ahmari, S.E., J. Buchanan, and S.J. Smith. 2000. Assembly of presynaptic active zones from cytoplasmic transport packets. *Nat. Neurosci.* 3:445–451.
- Burry, R.W. 1986. Presynaptic elements on artificial surfaces. A model for the study of development and regeneration of synapses. *Neurochem. Pathol.* 5:345–360.
- Burry, R.W. 1991. Transitional elements with characteristics of both growth cones and presynaptic terminals observed in cell cultures of cerebellar neurons. *J. Neurocytol.* 20:124–132.
- Clague, M.J. 1998. Molecular aspects of the endocytic pathway. *Biochem. J.* 336:271–282.
- Cremer, H., R. Lange, A. Christoph, M. Plomann, G. Vopper, J. Roes, R. Brown, S. Baldwin, P. Kraemer, S. Scheff, et al. 1994. Inactivation of the N-CAM gene in mice results in size reduction of the olfactory bulb and deficits in spatial learning. *Nature.* 367:455–459.
- Cochilla, A.J., J.K. Angleson, and W.J. Betz. 1999. Monitoring secretory membrane with FM1-43 fluorescence. *Annu. Rev. Neurosci.* 22:1–10.
- Dai, Z., and H.B. Peng. 1996. Dynamics of synaptic vesicles in cultured spinal cord neurons in relationship to synaptogenesis. *Mol. Cell. Neurosci.* 7:443–452.
- De Matteis, M.A., and J.S. Morrow. 2000. Spectrin tethers and mesh in the biosynthetic pathway. *J. Cell Sci.* 113:2331–2343.
- De Matteis, M.A., and J.S. Morrow. 1998. The role of ankyrin and spectrin in membrane transport and domain formation. *Curr. Opin. Cell Biol.* 10:542–549.
- Dityatev, A., G. Dityateva, and M. Schachner. 2000. Synaptic strength as a function of post- versus presynaptic expression of the neural cell adhesion molecule NCAM. *Neuron.* 26:207–217.
- Ethell, I.M., and Y. Yamaguchi. 1999. Cell surface heparan sulfate proteoglycan syndecan-2 induces the maturation of dendritic spines in rat hippocampal neurons. *J. Cell Biol.* 144:575–586.
- Fath, K.R., G.M. Trimbur, and D.R. Burgess. 1997. Molecular motors and a spectrin matrix associate with Golgi membranes in vitro. *J. Cell Biol.* 139:1169–1181.
- Featherstone, D.E., W.S. Davis, R.R. Dubreuil, and K. Broadie. 2001. *Drosophila* α- and β-spectrin mutations disrupt presynaptic neurotransmitter release. *J. Neurosci.* 21:4215–4224.
- Fiala, J.C., M. Feinberg, V. Popov, and K.M. Harris. 1998. Synaptogenesis via dendritic filopodia in developing hippocampal area CA1. *J. Neurosci.* 18:8900–8911.
- Friedman, H.V., T. Bresler, C.C. Garner, and N.E. Ziv. 2000. Assembly of new individual excitatory synapses: time course and temporal order of synaptic molecule recruitment. *Neuron.* 27:57–69.
- Fukuda, M. 1991. Lysosomal membrane glycoproteins. Structure, biosynthesis, and intracellular trafficking. *J. Biol. Chem.* 266:21327–21330.
- Gennarini, G., M. Hirn, H. Deagostini-Bazin, and C. Goridis. 1984. Studies on the transmembrane disposition of the neural cell adhesion molecule N-CAM. The use of liposome-inserted radioiodinated N-CAM to study its transbilayer orientation. *Eur. J. Biochem.* 142:65–73.
- Girotti, M., and G. Banting. 1996. TGN38-green fluorescent protein hybrid proteins expressed in stably transfected eukaryotic cells provide a tool for the real-time, in vivo study of membrane traffic pathways and suggest a possible role for ratTGN38. *J. Cell Sci.* 109:2915–2926.
- Haest, C.W., G. Plasa, D. Kamp, and B. Deuticke. 1978. Spectrin as a stabilizer of the phospholipid asymmetry in the human erythrocyte membrane. *Biochim. Biophys. Acta.* 509:21–32.
- Heimann, K., J.M. Percival, R. Weinberger, P. Gunning, and J.L. Stow. 1999. Specific isoforms of actin-binding proteins on distinct populations of Golgi-derived vesicles. *J. Biol. Chem.* 274:10743–10750.
- Hollenbeck, P.J. 1993. Products of endocytosis and autophagy are retrieved from axons by regulated retrograde organelle transport. *J. Cell Biol.* 121:305–315.
- Holleran, E.A., and E.L. Holzbaur. 1998. Speculating about spectrin: new insights into the Golgi-associated cytoskeleton. *Trends Cell Biol.* 8:26–29.
- Koenig, E., S. Kinsman, E. Repasky, and L. Sultz. 1985. Rapid mobility of motile varicosities and inclusions containing α-spectrin, actin, and calmodulin in regenerating axons *in vitro*. *J. Neurosci.* 5:715–729.
- Kraszewski, K., O. Mundigl, L. Daniell, C. Verderio, M. Matteoli, and P. De Camilli. 1995. Synaptic vesicle dynamics in living cultured hippocampal neurons visualized with CY3-conjugated antibodies directed against the luminal domain of synaptotagmin. *J. Neurosci.* 15:4328–4342.
- Lee, S.H., and M. Sheng. 2000. Development of neuron-neuron synapses. *Curr. Opin. Neurobiol.* 10:125–131.
- Lippincott-Schwartz, J. 1998. Cytoskeletal proteins and Golgi dynamics. *Curr. Opin. Cell Biol.* 10:52–59.
- Liu, G., and R.W. Tsien. 1995. Properties of synaptic transmission at single hippocampal synaptic boutons. *Nature.* 375:404–408.
- Lledo, P.M., X. Zhang, T.C. Sudhof, R.C. Malenka, and R.A. Nicoll. 1998. Postsynaptic membrane fusion and long-term potentiation. *Science.* 279:399–403.
- Maletic-Savatic, M., and R. Malinow. 1998. Calcium-evoked dendritic exocytosis in cultured hippocampal neurons. Part I: trans-Golgi network-derived organelles undergo regulated exocytosis. *J. Neurosci.* 18:6803–6813.
- Maletic-Savatic, M., T. Koethan, and R. Malinow. 1998. Calcium-evoked dendritic exocytosis in cultured hippocampal neurons. Part II: mediation by calcium/calmodulin-dependent protein kinase II. *J. Neurosci.* 18:6814–6821.
- Mallard, F., C. Antony, D. Tenza, J. Salamero, B. Goud, and L. Johannes. 1998. Direct pathway from early/recycling endosomes to the Golgi apparatus revealed through the study of shiga toxin B-fragment transport. *J. Cell Biol.* 143:973–990.
- Mammen, A.L., R.L. Huganir, and R.J. O'Brien. 1997. Redistribution and stabilization of cell surface glutamate receptors during synapse formation. *J. Neurosci.* 17:7351–7358.
- Martini, R., and M. Schachner. 1986. Immunoelectron microscopic localization of neural cell adhesion molecules (L1, N-CAM, and MAG) and their shared carbohydrate epitope and myelin basic protein in developing sciatic nerve. *J. Cell Biol.* 103:2439–2448.
- Matteoli, M., K. Takei, M.S. Perin, T.C. Sudhof, and P. De Camilli. 1992. Exo-endocytic recycling of synaptic vesicles in developing processes of cultured hippocampal neurons. *J. Cell Biol.* 117:849–861.

- McKiernan, A.E., R.I. MacDonald, R.C. MacDonald, and D. Axelrod. 1997. Cytoskeletal protein binding kinetics at planar phospholipid membranes. *Biophys. J.* 73:1987–1998.
- Mu, F.T., J.M. Callaghan, O. Steele-Mortimer, H. Stenmark, R.G. Parton, P.L. Campbell, J. McCluskey, J.P. Yeo, E.P. Tock, and B.H. Toh. 1995. EEA1, an early endosome-associated protein. EEA1 is a conserved  $\alpha$ -helical peripheral membrane protein flanked by cysteine “fingers” and contains a calmodulin-binding IQ motif. *J. Biol. Chem.* 270:13503–13511.
- Overly, C.C., H.I. Rieff, and P.J. Hollenbeck. 1996. Organelle motility and metabolism in axons vs dendrites of cultured hippocampal neurons. *J. Cell Sci.* 109:971–980.
- Nakata, T., S. Terada, and N. Hirokawa. 1998. Visualization of the dynamics of synaptic vesicle and plasma membrane proteins in living axons. *J. Cell Biol.* 140:659–674.
- Paglini, G., L. Peris, F. Mascotti, S. Quiroga, and A. Caceres. 2000. Tau protein function in axonal formation. *Neurochem. Res.* 25:37–42.
- Papa, M., M.C. Bundman, V. Greenberger, and M. Segal. 1995. Morphological analysis of dendritic spine development in primary cultures of hippocampal neurons. *J. Neurosci.* 15:1–11.
- Polishchuk, R.S., E.V. Polishchuk, P. Marra, S. Alberti, R. Buccione, A. Luini, and A.A. Mironov. 2000. Correlative light-electron microscopy reveals the tubular-saccular ultrastructure of carriers operating between Golgi apparatus and plasma membrane. *J. Cell Biol.* 148:45–58.
- Pollerberg, G.E., M. Schachner, and J. Davoust. 1986. Differentiation state-dependent surface mobilities of two forms of the neural cell adhesion molecule. *Nature.* 324:462–465.
- Pollerberg, G.E., K. Burridge, K.E. Krebs, S.R. Goodman, and M. Schachner. 1987. The 180-kD component of the neural cell adhesion molecule N-CAM is involved in a cell-cell contacts and cytoskeleton-membrane interactions. *Cell Tissue Res.* 250:227–236.
- Polo-Parada, L., C.M. Bose, and L.T. Landmesser. 2001. Alterations in transmission, vesicle dynamics, and transmitter release machinery at NCAM-deficient neuromuscular junctions. *Neuron.* 32:815–828.
- Rao, A., E. Kim, M. Sheng, and A.M. Craig. 1998. Heterogeneity in the molecular composition of excitatory postsynaptic sites during development of hippocampal neurons in culture. *J. Neurosci.* 18:1217–1229.
- Robinson, M.S., and T.E. Kreis. 1992. Recruitment of coat proteins onto Golgi membranes in intact and permeabilized cells: effects of brefeldin A and G protein activators. *Cell.* 69:129–138.
- Ryan, T.A., H. Reuter, B. Wendland, F.E. Schweizer, R.W. Tsien, and S.J. Smith. 1993. The kinetics of synaptic vesicle recycling measured at single presynaptic boutons. *Neuron.* 11:713–724.
- Scheiffele, P., J. Fan, J. Choih, R. Fetter, and T. Serafini. 2000. Neuroligin expressed in nonneuronal cells triggers presynaptic development in contacting axons. *Cell.* 101:657–669.
- Schmid, S.L. 1997. Clathrin-coated vesicle formation and protein sorting: an integrated process. *Annu. Rev. Biochem.* 66:511–548.
- Schuster, C.M., G.W. Davis, R.D. Fetter, and C.S. Goodman. 1996. Genetic dissection of structural and functional components of synaptic plasticity. I. Fasciclin II controls synaptic stabilization and growth. *Neuron.* 17:641–654.
- Shafit-Zagardo, B., and N. Kalcheva. 1998. Making sense of the multiple MAP-2 transcripts and their role in the neuron. *Mol. Neurobiol.* 16:149–162.
- Shepherd, G.M., and K.M. Harris. 1998. Three-dimensional structure and composition of CA3/ECA1 axons in rat hippocampal slices: implications for presynaptic connectivity and compartmentalization. *J. Neurosci.* 18:8300–8310.
- Shi, S.H., Y. Hayashi, R.S. Petralia, S.H. Zaman, R.J. Wenthold, K. Svoboda, and R. Malinow. 1999. Rapid spine delivery and redistribution of AMPA receptors after synaptic NMDA receptor activation. *Science.* 284:1811–1816.
- Sikorski, A.F., and M. Kuczek. 1985. Labelling of erythrocyte spectrin in situ with phenylisothiocyanate. *Biochim. Biophys. Acta.* 820:147–153.
- Sonnichsen, B., S. De Renzis, E. Nielsen, J. Rietdorf, and M. Zerial. 2000. Distinct membrane domains on endosomes in the recycling pathway visualized by multicolor imaging of Rab4, Rab5, and Rab11. *J. Cell Biol.* 149:901–914.
- Stephens, D.J., and R. Pepperkok. 2001. Illuminating the secretory pathway: when do we need vesicles? *J. Cell Sci.* 114:1053–1059.
- Tarabal, O., J. Caldero, J. Llado, R.W. Oppenheim, and J.E. Esquerda. 2001. Long-lasting aberrant tubulovesicular membrane inclusions accumulate in developing motoneurons after a sublethal excitotoxic insult: a possible model for neuronal pathology in neurodegenerative disease. *J. Neurosci.* 21:8072–8081.
- Toomre, D., P. Keller, J. White, J.C. Olivo, and K. Simons. 1999. Dual-color visualization of trans-Golgi network to plasma membrane traffic along microtubules in living cells. *J. Cell Sci.* 112:21–33.
- Toomre, D., J.A. Steyer, P. Keller, W. Almers, and K. Simons. 2000. Fusion of constitutive membrane traffic with the cell surface observed by evanescent wave microscopy. *J. Cell Biol.* 149:33–40.
- Washbourne, P., J.E. Bennett, and A.K. McAllister. 2002. Rapid recruitment of NMDA receptor transport packets to nascent synapses. *Nat. Neurosci.* 5:751–759.
- Zakharenko, S., S. Chang, M. O’Donoghue, and S.V. Popov. 1999. Neurotransmitter secretion along growing nerve processes: comparison with synaptic vesicle exocytosis. *J. Cell Biol.* 144:507–518.
- Zhai, R.G., H. Vardinon-Friedman, C. Cases-Langhoff, B. Becker, E.D. Gundelfinger, N.E. Ziv, and C.C. Garner. 2001. Assembling the presynaptic active zone: a characterization of an active one precursor vesicle. *Neuron.* 29:131–143.